International Journal of Heat and Mass Transfer 85 (2015) 647–655

Contents lists available at ScienceDirect

International Journal of Heat and Mass Transfer

journal homepage: www.elsevier.com/locate/ijhmt

Population balance modeling for the charging process of a PCM cold energy storage tank

Jing Wu [a], Emilie Gagnière [a], Frédéric Jay [b], Christian Jallut [a,*]

[a] Université de Lyon, Université Lyon 1, Laboratoire d'Automatique et de Génie des Procédés, UMR 5007, CNRS/UCBL, 43 Bd du 11 Novembre 1918, 69622 Villeurbanne Cedex, France
[b] CRISTOPIA Energy Systems, 78 chemin du Moulin de la Clue, Quartier Cayregues, 06140 Vence, France

ARTICLE INFO

Article history:
Received 4 November 2014
Received in revised form 5 February 2015
Accepted 6 February 2015

Keywords:
Population balance equations
Energy storage
Phase change material
Supercooling

ABSTRACT

In this paper, a dynamic model is proposed for the charging process of a cold energy storage made of a fixed bed of spherical nodules containing a Phase Change Material (PCM). During the charging process, even if the temperature of the cooling liquid that flows through the storage is uniform, the solidification process does not begin at the same temperature among the nodules due to the supercooling phenomenon. A first number distribution can be defined according to the solid mass fraction among the nodules experiencing solidification. At the end of the solidification process, the temperature of the solid phase is not the same among the nodules population having completed the solidification. A second number distribution can be defined according to their mean temperature. In order to calculate the time evolution of these two number distributions, we propose to use the population balance equation approach coupled with nodules energy balance equations. The resulting partial differential equations are spatially discretized by the finite difference method. The supercooling phenomenon is taken into account as a boundary condition of the population balance equation associated with the solid mass fraction by using a nucleation kinetic model. The resulting set of ordinary differential equations is numerically solved. The model is applied for simulating the charge cycle of an ice storage system. Good agreement between simulation results and experimental data is achieved.

1. Introduction

Thermal energy storage using the solidification/fusion enthalpy of Phase Change Materials (PCM) is considered as an effective and sustainable tool for energy use owing to its energy storage high density and low CO_2 emission [1,2]. The large amount of heat that can be exchanged during the phase change processes permits to make containers small in size. Cold energy storage with PCM has recently been studied for shifting electricity consumption from pick hours in Heating, Ventilation and Air-Conditioning (HVAC) applications [3–5]. The PCM is solidified by a chiller when the buildings cooling demand is low, whereas the storage operates in parallel with the chiller when the cooling demand is high.

Modeling PCM storage systems is important since it helps to make predictions during operations for design and control purposes. An accurate and efficient model can be used to evaluate the thermal behavior and thus to reduce the time and expense of experimentation. Numerous models of PCM thermal storage systems are available in the literature, some of them being reviewed by Dutil et al. [6], Verma and Singal [7] and Liu et al. [8]. Developing a detailed model to characterize the thermal behavior of PCM thermal energy storages is complex due to the heat transfer problems associated to phase change and to the supercooling phenomenon [2,6].

Ismail and Henriquez [9] developed a numerical model for a storage system composed of a cylindrical tank and spherical nodules filled with water, using a finite difference approach and moving grid technique. In this model the heat transfer inside the nodules is calculated by using one-dimensional heat conduction model, and the natural convection between the PCM and the envelope is neglected. Bilir and Ilken [10] presented a numerical study on the inward solidification of a liquid PCM encapsulated in a cylindrical/spherical container. The governing equations are formulated and solved with control volume approach. The solid volume fraction is used to characterize the variations of the phase change front. Bony and Citherlet [11] realized a numerical and experimental study on the heat transfer in PCM plunged in water tank storage. An effective conduction coefficient approach is used to take into account for the internal convection inside PCM nodules. Zsembinszki et al. [3] developed a two-dimensional model for simulating the melting process of a cold storage tank filled with

* Corresponding author. Tel.: +33 4 72 431835.
E-mail address: jallut@lagep.univ-lyon1.fr (C. Jallut).

http://dx.doi.org/10.1016/j.ijheatmasstransfer.2015.02.012
0017-9310/

Nomenclature

A	pre-exponential factor (s^{-1})
a	thermal diffusivity ($m^2\ s^{-1}$)
c_p	specific heat capacity ($J\ K^{-1}\ kg^{-1}$)
CSTR	Continuous Stirred Tank Reactor
D	diameter (m)
$\boldsymbol{f}$	flux
H	height (m)
I	probability of crystallization per unit time and volume ($m^{-3}\ s^{-1}$)
J	probability of crystallization per unit time (s^{-1})
k	thermal equivalent conductance (s^{-1})
K	Boltzmann constant ($J\ K^{-1}$)
m	mass (kg)
q	mass flow rate ($kg\ s^{-1}$)
n	number of nodules
N	number of discrete elements
Nu	Nusselt number
p	source term per unit volume in a balance equation ($-m^{-3}\ s^{-1}$)
Pr	Prandtl number
r	nodule radius (m)
R	thermal resistance ($K\ W^{-1}$)
Re	Reynolds number
S	surface area of capsule (m^2)
T	temperature (K)
T_m	melting temperature (K)
t	time (s)
u	fluid velocity ($m\ s^{-1}$)
v	phase space velocity
x	solid mass fraction

Greek symbols

α	heat transfer coefficient ($W\ m^{-2}\ K^{-1}$)
β	extensity density ($-m^{-3}$)
γ	solidification level
ΔA^*	potential barrier for nucleation (J)
Δh_{sl}	enthalpy of fusion per unit of mass ($J\ kg^{-1}$)
λ	thermal conductivity ($W\ m^{-1}\ K^{-1}$)
μ	fluid dynamic viscosity (Pa s)
ρ	mass density ($kg\ m^{-3}$)
σ_{sl}	solid-liquid interfacial tension ($N\ m^{-1}$)
ϕ	heat flux (W)
ψ_x	number density at a certain solid mass fraction
ψ_{T_s}	number density at a certain solid temperature (K^{-1})

Subscripts

c	capsule
d	two phase
e	outside of nodules
env	envelope of nodules
f	cooling fluid
i	inside of nodules
k	kth CSTR
l	liquid
s	solid
$\boldsymbol{R}$	spatial coordinates
t	total
$\boldsymbol{Z}$	phase space coordinates

commercial PCM flat slabs. They used the implicit finite difference method for solving the energy balance equations of nodules and heat transfer fluid. Votyakov and Bonanos [12] applied the perturbation theory to predict the performance of packed bed thermocline thermal energy storage tanks. Their work is based upon a one-dimensional one-phase model, in neglecting heat conduction in the solid filler and in the fluid, and assuming a lumped heat capacitance model.

During a cooling process, a liquid PCM does not generally crystallize immediately when the temperature reaches its melting temperature, whereas there is no delay when a solid PCM melts. In order to achieve the solidification process, the liquid PCM has to be supercooled. The supercooling phenomenon is characterized by the difference between the melting temperature and the average temperature at which the liquid starts to crystallise. It can significantly increase the storage charging duration and the load of refrigeration systems, so it is important to account for the phenomenon in dynamic modeling of thermal energy storages [13,14].

As far as we know, only few authors have taken into consideration the supercooling phenomenon in dynamic modeling of thermal energy storage systems: Wu et al. [15] and Calvet et al. [16] assumed that the PCM has a constant solidifying temperature which is less than the melting temperature. The solidifying temperature is fixed at an average value determined by experimental tests. It is a simplified approach since the PCM does not always crystallize at the same temperature according to experimental investigations [17]. Bédécarrats et al. [18] proposed to use the probability of crystallization per unit time, a concept originated from the conventional theory of nucleation, to account for the stochastic character of the freezing process due to the supercooling phenomenon. This approach has proven to be efficient and accurate in predicting the thermal behavior of PCM storages [19,20]. A theoretical and experimental investigation is presented by El Rhafiki et al. [21] for characterizing the probability of crystallization of PCMs inside an emulsion.

In this paper, we propose to use the population balance equation approach to derive a dynamic model of the charging process of a cold energy thermal storage, which is made of a fixed bed of spherical nodules containing a PCM. This framework allows describing in a simple and elegant way the influence of the supercooling phenomenon by introducing two number distributions among the nodules. The first one allows describing the repartition of nodules the content of which is experiencing solidification: this repartition is defined as a function of the solid mass fraction and time. The second one allows describing the repartition of nodules the content of which is solid and is experiencing solid phase cooling: this repartition is defined as a function of the solid mean temperature and time. To our better knowledge, at present no applications of the population balance equations approach to thermal storage modeling are available in the literature.

This paper is organized as follows. An introduction to the principle of the population balance equations is presented in Section 2. A novel thermal energy storage model based on the population and energy balance equations that we propose in this work is described in Section 3. Simulation results and comparison with experimental data are presented in Section 4 and finally conclusions are given in Section 5.

2. Principle of the population balance equations

The general form of the balance equation for a scalar extensive quantity is very well described in numerous textbooks (see for example [22]):

$$\frac{\partial \beta}{\partial t} + \nabla_{\boldsymbol{R}} \cdot \boldsymbol{f}_{\boldsymbol{R}} = p \tag{1}$$

where β is the volumetric density, $\boldsymbol{f}_{\boldsymbol{R}}$ is the flux and p is the volumetric source term. The divergence operator $\nabla_{\boldsymbol{R}}\cdot$ is taken over the spatial coordinates $\boldsymbol{R} = [R_1 \quad R_2 \quad R_3]^T$. A population balance equation can be considered as an extension of an ordinary balance equation to a supplementary coordinates vector $\boldsymbol{Z} = [Z_1 \quad Z_2 \quad \ldots]^T$, which represents some properties or phase variables associated to the extensive quantity that is counted [23]. The latter is discrete in nature so that a number density function $\psi(\boldsymbol{R}, \boldsymbol{Z}, t)$ can be defined as follows:

$$dn = \psi(\boldsymbol{R}, \boldsymbol{Z}, t) dR_1 dR_2 dR_3 dZ_1 dZ_2 \ldots \tag{2}$$

dn is the number of discrete entities being in the elementary spatial volume $dR_1 dR_2 dR_3$ and having their properties Z_j included in the intervals $[Z_j, Z_j + dZ_j]$. The flux in the phase space is generally considered as purely convective so that the total flux $\boldsymbol{f}$ is given by:

$$\boldsymbol{f} = \boldsymbol{v}_{\boldsymbol{Z}} \psi + \boldsymbol{f}_{\boldsymbol{R}} \tag{3}$$

where $\boldsymbol{v}_{\boldsymbol{Z}}$ is the velocity in the phase space. A population balance equation is then as follows:

$$\frac{\partial \psi}{\partial t} + \nabla_{\boldsymbol{Z}} \cdot [\boldsymbol{v}_{\boldsymbol{Z}} \psi] + \nabla_{\boldsymbol{R}} \cdot \boldsymbol{f}_{\boldsymbol{R}} = p \tag{4}$$

The volumetric source term p includes death and birth processes as well as breakage and agglomeration ones. The latter are represented by integrals involving specific kernels.

Population balance equations approach has been widely used for modeling particulate processes such as suspension polymerization [24], crystallization [25] and emulsification [26] for example. In the case of anisotropic particles crystallization, a distribution defined over two property phase variables like length and width can be used [27,28]. If the volumetric density function does not depend on the spatial position $\boldsymbol{R}$, the population balance equation is reduced to:

$$\frac{\partial \psi}{\partial t} + \nabla_{\boldsymbol{Z}} \cdot [\boldsymbol{v}_{\boldsymbol{Z}} \psi] = p \tag{5}$$

For example, this assumption corresponds to the case of a perfectly mixed or mixed-suspension, mixed-product-removal crystallizer [27].

3. Application to a PCM thermal storage modeling

3.1. Thermal storage principle

The general vertical tank configuration of a cold energy storage system is shown in Fig. 1. It is composed of a cylindrical tank filled with a fixed bed of spherical nodules containing the PCM and a cooling fluid flowing through the bed. Diffusers that are placed inside the tank ensure that the cooling fluid is homogeneously dispatched on all the tank section. The heat transfer is carried out by the contact between the nodules and the fluid. The inlet cooling fluid temperature is controlled by a refrigeration loop. During the charging process, the cooling fluid enters from the bottom of the tank and flows through the PCM nodules. The cooling fluid inlet temperature is lower than the PCM melting temperature so that the initially liquid PCM is gradually cooled and then releases heat through solidification.

Finally, the nodules solid content temperature decreases after the freezing process is completed. During the discharging process, warmer fluid is supplied from the top so that the PCM melts.

3.2. Global structure of the model

The cooling fluid flow is assumed to be equivalent to a cascade of N identical Continuous Stirred Tank Reactors. In the sequel, we describe the elementary sub-model that we propose for the kth Continuous Stirred Tank Reactors ($k = 1 \ldots N$), the complete model being a serial interconnection of N elementary sub-models. A population of nodules is associated to the kth Continuous Stirred Tank Reactor as shown in Fig. 2.

Let us consider the cooling and freezing processes of the content of these nodules. From the definition of a Continuous Stirred Tank Reactor, the cooling fluid temperature is uniform so that it is only a function of time $T_f^k(t)$. At the beginning of the charging process, the nodules content is liquid. If the cooling fluid temperature is sufficiently low, the freezing process begins in some nodules whereas the content of the others remains liquid due to the supercooling phenomenon. It has been experimentally found that once the freezing process has begun in a nodule, the temperature of its content reaches immediately the melting temperature T_m and it remains constant as the solid mass fraction x increases until the nodule content to be totally solid [16]. From that point, the solid phase temperature begins to decrease according to the cooling fluid temperature. Since the freezing process does not begin at the same time in all the nodules, it does not stop at the same time either. Due to this global freezing process, the total number of nodules within the kth Continuous Stirred Tank Reactor under consideration, that is denoted by n_t^k, can be decomposed into the sum of three terms at each time t:

$$n_t^k = n_d^k(t) + n_s^k(t) + n_l^k(t) = cte \tag{6}$$

$n_d^k(t)$ is the number of nodules containing a mixture of liquid and solid. Since the freezing process does not begin at the same time in all the nodules, a number density function $\psi_x^k(x,t)$ can be defined that is assumed to depend on the solid mass fraction and the time:

$$\begin{cases} dn_d^k = \psi_x^k(x,t)dx \\ n_d^k(t) = \int_\varepsilon^1 \psi_x^k(x,t)dx \end{cases} \tag{7}$$

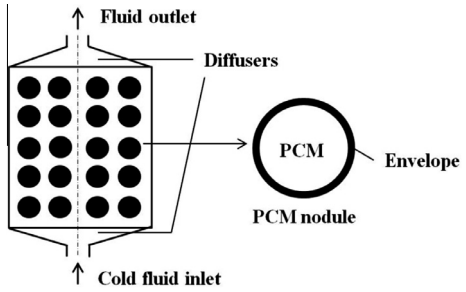

Fig. 1. Charging configuration of cold energy storage system.

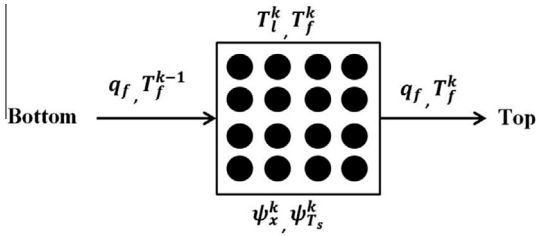

Fig. 2. Scheme of the kth Continuous Stirred Tank Reactor and the associated nodules.

dn_d^k is the number of nodules containing a mixture of liquid and solid having a solid mass fraction between x and $x+dx$ at time t. The normalization condition gives the total number of nodules $n_d^k(t)$. ε is the value of x at the beginning of the freezing process, which is determined in Section 3.4.

$n_s^k(t)$ is the number of nodules containing a solid phase. Let us define T_s as the mean value of the solid phase temperature within a nodule. This temperature is not the same among all the nodules containing a solid phase since the freezing process does not begin and stop at the same time in all the nodules. A number density function $\psi_{T_s}^k(T_s,t)$ can be defined that is assumed to depend on the mean solid temperature and the time:

$$\begin{cases} dn_s^k = \psi_{T_s}^k(T_s,t)dT_s \\ n_s^k(t) = \int_{T_{s,\min}}^{T_m} \psi_{T_s}^k(T_s,t)dT_s \end{cases} \tag{8}$$

dn_s^k is the number of nodules containing a solid phase having a mean temperature between T_s and T_s+dT_s at time t. The normalization condition gives the total number of nodules $n_s^k(t)$ of which the mean temperature is necessarily lower than the melting temperature T_m. A lowest value of T_s, denoted by $T_{s,\min}$, can be defined according to the final value of the cooling fluid temperature.

$n_l^k(t)$ is the number of nodules containing a liquid phase. T_l^k is the mean value of the liquid phase temperature within a nodule. Due to the way the charging process is performed, the content of all the nodules containing a liquid phase is assumed to have the same mean temperature so that it is not necessary to define any density function for this population.

3.3. Population balance equations

The number densities ψ_x^k and $\psi_{T_s}^k$ are assumed to be independent of the spatial position in the kth Continuous Stirred Tank Reactor so that Eq. (5) applies. Since the storage contains separated nodules, the population balance equations do not contain any breakage or agglomeration terms.

The population balance equation related to the nodules containing a mixture of liquid and solid is:

$$\frac{\partial\psi_x^k(x,t)}{\partial t} + \frac{\partial(v_x^k\psi_x^k(x,t))}{\partial x} = 0 \tag{9}$$

The source term is equal to zero since the birth of nodules containing PCM beginning to solidify occurs only at a tiny value of x: this phenomenon is treated as a boundary condition of Eq. (9) (see Section 3.4). No death occurs, once a crystal has begun to grow within a nodule, the process continues until the nodule content is totally solidified. This phenomenon is also treated as a boundary condition (see Section 3.4).

The velocity in the solid mass fraction space v_x^k is given by the energy balance equation of one nodule content during the solidification process:

$$m_c\Delta h_{sl}\frac{dx^k}{dt} = m_c\Delta h_{ls}v_x^k = \phi_x^k = \frac{\left(T_m - T_f^k\right)}{R_d^k} \tag{10}$$

R_d^k is the global heat transfer resistance during the solidification process, m_c is the nodule content mass and Δh_{sl} the PCM fusion enthalpy. In Eq. (10), the nodule content temperature is assumed to be uniform and equal to the melting temperature according to available experimental results [16].

In the same manner, the population balance equation related to the nodules containing solid phase is:

$$\frac{\partial\psi_{T_s}^k(T_s,t)}{\partial t} + \frac{\partial(v_{T_s}^k\psi_{T_s}^k(T_s,t))}{\partial T_s} = 0 \tag{11}$$

The source term is also equal to zero since the birth of nodules containing newly totally solidified PCM occurs only at the melting temperature: this phenomenon is also treated as a boundary condition of Eq. (11) (see Section 3.4). No death occurs, once the solid phase temperature has begun to decrease in a nodule, the process continues according to the cooling fluid temperature.

The velocity in the mean solid temperature space $v_{T_s}^k$ is also given by the energy balance equation of the nodule content during the solid phase cooling:

$$m_c c_{ps}\frac{dT_s^k}{dt} = m_c c_{ps}v_{T_s}^k = -\phi_s^k = \frac{\left(T_f^k - T_s^k\right)}{R_s^k} \tag{12}$$

R_s^k is the global heat transfer resistance during the solid phase cooling process, c_{ps} is the solid phase heat capacity.

3.4. Population balance equations initial and boundary conditions

We simulate a charge cycle where the initial PCM state is liquid within all the nodules, so that:

$$\psi_s^k(x,t=0) = 0 \tag{13}$$

$$\psi_{T_s}^k(T_s,t=0) = 0 \tag{14}$$

Due to the supercooling phenomenon, the solidification process leads to the formation of very small nuclei within the nodules at a temperature lower than the melting temperature. According to the work carried out by Bédécarrats et al. [18], the birth rate of nodules containing a first nucleus can be derived from the conventional theory of nucleation as a first order process with respect to the number of nodules containing liquid phase:

$$r_{nuc} = J(T_l)n_l \tag{15}$$

where T_l is the temperature of the supercooled liquid, $J(T_l)$ is the so-called probability of crystallization per unit time.

The general formula for the probability of crystallization per unit time and per unit volume is [29]:

$$I(T_l) = A(T_l)\exp\left(-\frac{\Delta A*}{KT_l}\right) \tag{16}$$

where K is the Boltzmann constant, ΔA^* is the potential barrier for nucleation:

$$\Delta A^* = \frac{16\pi\sigma_{sl}^2}{3(\rho_s\Delta h_{sl})^2}\left(\frac{T_m}{T_m - T_l}\right)^2 \tag{17}$$

with σ_{sl} being the solid–liquid interfacial tension and ρ_s the mass density of the crystal.

The pre-exponential factor $A(T_l)$ in Eq. (16) varies slower than the exponential term and can thus be considered as a constant [21]. For a given volume, the probability of crystallization per unit time can be expressed as:

$$J(T_l) = a\exp\left(-\frac{b}{T_l(T_m - T_l)^2}\right) \tag{18}$$

The main assumption that is taken to derive Eq. (15) is that there is only one nucleus per nodule. This assumption is similar to the one that is taken for the modeling of crystallization in emulsions for example [30].

The flux of nodules entering the population containing a solid–liquid mixture at a very small quantity of solid phase characterized by the smallest mass fraction ε is then related to the nucleation rate according to the following boundary condition:

$$\psi_x^k(x=\varepsilon,t)\,v_x^k(x=\varepsilon,t) = J(T_l^k)n_l^k \tag{19}$$

As it has been pointed out in [16], once the solidification process has begun in a nodule, the temperature reaches very rapidly the melting temperature. This process can be considered to be adiabatic and the value of ε can be calculated by solving the following energy balance:

$$h_l(T_{l,c}) = \varepsilon h_s(T_m) + (1-\varepsilon)h_l(T_m) \tag{20}$$

where h_l and h_s are respectively the liquid and solid phase specific enthalpy. $T_{l,c}$ is the liquid phase temperature at which the crystallization begins.

From the balance Eq. (20), it is easy to derive the following expression if the liquid phase heat capacity c_{pl} is assumed to be constant:

$$\varepsilon = \frac{c_{pl}(T_m - T_{l,c})}{\Delta h_{sl}} \tag{21}$$

In the case of water, $1.25\% < \varepsilon < 7.53\%$ for $1\,^\circ\text{C} < (T_m - T_{l,c}) < 6\,^\circ\text{C}$. As a consequence, a mean constant value can be taken for ε: $\varepsilon = 0.0253$.

The flux of nodules leaving the population containing a solid–liquid mixture at $x = 1$ is equal to the flux of nodules entering the population of nodules containing solid phase at $T_s = T_m$ since the solidification process temperature is constant and equal to the melting temperature. The boundary condition for $\psi^k_{T_s}$ is then:

$$\psi^k_{T_s}(T_s = T_m, t)\, v^k_{T_s}(T_s = T_m, t) = -\psi^k_x(x = 1, t)\, v^k_x(x = 1, t) \tag{22}$$

3.5. Model of the nodules containing liquid phase

The variation of the number of nodules containing liquid phase is given by the following balance equation:

$$\frac{dn^k_l}{dt} = -J\left(T^k_l\right) n^k_l \tag{23}$$

Due to the initial conditions (13) and (14), $n_d(0) = n_s(0) = 0$ so that according to Eq. (6), the initial condition for n^k_l is:

$$n^k_l(0) = n^k_t \tag{24}$$

In order to calculate the evolution of the mean temperature of nodules containing liquid phase, we use the following energy balance of a nodule and the associated initial condition:

$$\begin{aligned} m_c c_{pl} \frac{dT^k_l}{dt} &= -\phi^k_l = \frac{\left(T^k_f - T^k_l\right)}{R^k_l} \\ T^k_l(0) &= T^k_{l,0} \end{aligned} \tag{25}$$

where R^k_l is the global heat transfer resistance during the liquid phase cooling process.

3.6. Continuous Stirred Tank Reactor cooling fluid model

The kth Continuous Stirred Tank Reactor inlet and outlet cooling fluid mass flow rates are identical. In order to calculate the kth Continuous Stirred Tank Reactor cooling fluid temperature, one has to solve the following energy balance:

$$\begin{aligned} m_f c_{pf} \frac{dT^k_f}{dt} = q_f c_{pf}\left(T^{k-1}_f - T^k_f\right) + n^k_l \phi^k_l + \int_\varepsilon^1 \psi^k_x(x,t)\phi^k_x dx \\ + \int_{T_{s,\min}}^{T_m} \psi^k_{T_s}(T_s,t)\phi^k_s dT_s \end{aligned} \tag{26}$$

where m_f is the cooling fluid constant mass of each CSTR, c_{pf} is the cooling fluid heat capacity that is assumed to be constant, T^{k-1}_f is the cooling fluid kth Continuous Stirred Tank Reactor inlet temperature that is the cooling fluid outlet temperature of the $(k-1)^{\text{th}}$ ones. As a matter of fact, due to the definition of a Continuous Stirred Tank Reactor, its outlet fluid temperature is equal to the fluid temperature inside the Continuous Stirred Tank Reactor. In Eq. (26), we have assumed that the storage tank heat losses are negligible. The last three terms of the right-hand side of Eq. (26) are the heat fluxes that are exchanged respectively with the nodules containing a liquid phase, a mixture of liquid and solid and a solid phase.

3.7. Determination of the nodule global heat transfer resistances

The heat exchange between the PCM and the fluid can be characterized by a series of three heat transfer resistances: the external convective resistance between the nodule envelope and the cooling fluid, the conductive resistance within the nodule envelope and the resistance within the PCM.

In order to calculate the external heat transfer coefficient, the correlation proposed by Wakao and Kaguei [31] for flows through fixed beds of spheres is used:

$$Nu = \frac{\alpha_e 2r_e}{\lambda_f} = 2.0 + 1.1 Pr^{1/3} Re^{0.6} \tag{27}$$

The conductive resistance of the nodule envelope that is assumed to operate at steady state is:

$$R_{env} = \frac{1}{4\pi\lambda_{env}}\left(\frac{1}{r_i} - \frac{1}{r_e}\right) \tag{28}$$

As far as the heat transfer within the PCM is concerned, one has to consider three configurations: the PCM is entirely solid, entirely liquid or a mixture of liquid and solid.

Zhu and Zhang [32] have proposed an empirical correlation for the equivalent heat transfer coefficient within the PCM during the solidification process that we use here:

$$\alpha_{i,d} = 69 - 27.8x - 128.9x^2 + 95.8x^3 \tag{29}$$

where x is the solid mass fraction.

Let us now consider the heat transfer within a solid PCM, which is purely conductive. In order to calculate the mean solid phase temperature T_s, we propose to use the so-called Linear Driving Force model that is extensively applied in the domain of adsorption processes modeling [33,34]. This model has been proposed by Glueckauf [35] to describe transient diffusion within spheres. If we transpose the Linear Driving Force model to conductive transient heat transfer (see the Appendix A), the mean value of the solid phase temperature can be accurately calculated by solving the following simplified energy balance:

$$\frac{dT_s}{dt} = k_s(T_i - T_s) = \frac{\alpha_{is} S_i}{m_c c_{ps}}(T_i - T_s) \tag{30}$$

T_i is the temperature of the sphere surface and k_s is an equivalent conductance that is given by [33,35]:

$$k_s = \frac{15 a_s}{r_i^2} \tag{31}$$

where a_s is the solid thermal diffusivity.

We can also apply this model when the PCM is totally liquid to calculate the nodule content mean temperature T_l:

$$\begin{aligned} \frac{dT_l}{dt} &= k_l(T_i - T_l) = \frac{\alpha_{il} S_i}{m_c c_{pl}}(T_i - T_l) \\ k_l &= \frac{15 a_l}{r_i^2} \end{aligned} \tag{32}$$

Since convective contribution can exist within the liquid phase, the liquid phase thermal diffusivity a_l can be replaced by an equivalent one as suggested in [11].

Finally, the total resistance to heat transfer within the nodules are given by the following equations according to the three configurations:

$$R_s = \frac{1}{S_e\alpha_e} + R_{env} + \frac{1}{S_i\alpha_{is}}$$
$$R_l = \frac{1}{S_e\alpha_e} + R_{env} + \frac{1}{S_i\alpha_{il}} \quad (33)$$
$$R_d = \frac{1}{S_e\alpha_e} + R_{env} + \frac{1}{S_i\alpha_{id}}$$

3.8. Numerical solution of the model

The population balance Eqs. (9), (11) and the associated boundary conditions (19) and (22) are spatially discretized by using the finite difference technique. In combination with Eqs. (10), (12), (23), (25) and (26), we obtain an ordinary differential equations system that is solved numerically by using the fourth-fifth order Runge–Kutta method with adaptive step size.

4. Model simulation and validation

4.1. Simulation conditions

In Table 1 are given the values of the main parameters that are used for the simulations. The detailed test facility description and experimental data were published by Bédécarrats et al. [36].

The investigated PCM is water/ice with melting temperature $T_m = 0\,^{\circ}C$. The cooling fluid is an aqueous solution containing 30% of ethylene glycol by volume. The measured cooling fluid flow rate and inlet fluid temperature are used as input conditions for the model. We have considered that the cooling fluid flow is equivalent to a cascade of 10 Continuous Stirred Tank Reactors.

4.2. Estimation of a and b and sensitivity analysis to the nucleation rate model

The values of J or those of the parameters a and b in Eq. (18) are generally determined by curve fitting from specific experiments. For example, in order to estimate the values of J in the case of crystallization in emulsions, Kashiev et al. [30] have used experimental values of the velocity of ultrasounds in oil-in-water emulsion obtained during isothermal crystallization experiments while El Rhafiki et al. [21] have used Differential Scanning Calorimetry (DSC) technique. Bédécarrats et al. [18] have fitted a and b from isothermal crystallization experiments in a batch cooling system containing nodules similar to ones considered here.

In this work, the parameters a and b are estimated in order that the calculated storage fluid outlet temperature to be as close as possible to the measured one. The best fit that has been obtained is shown in Fig. 3 for $a = a^* = 0.198\ s^{-1}$ and $b = b^* = 8350\ K^3$. The model provides a good agreement between the predicted and measured outlet temperatures.

The deviations are less than 5%, they may result from the inaccuracy of heat transfer coefficients. We observe that the inlet and outlet temperatures fall off sharply during the liquid phase cooling in the beginning, and then they are stabilized at −5 °C and −2 °C respectively which correspond the solidification step. From 11 h the temperatures begin to decrease smoothly again, indicating the existence of entirely solidified nodules.

In order to test the sensitivity of the model to the nucleation rate model, different values of a and b (see Eq. (18)) are used to see their influence on the probability of crystallization (Fig. 4) and on the calculated cooling fluid outlet temperature (Fig. 5).

As shown in Fig. 4, the main influence of the a parameter is on the intensity of J, that is to say the liquid PCM probability to begin solidification is increased with a greater value of a. The b parameter not only affects the intensity of J but also significantly affects the temperature from which the PCM begins significantly to solidify. With a lower value of b, more liquid PCM will begin to solidify at a higher temperature.

As indicated in Fig. 5, the model is rather insensitive to the coefficient a, which has just a sight impact on the temperature of the turning point (at about 3 h). The coefficient b has a more considerable influence on the model, according to the results shown in Fig. 4. The variation of b shifts the curve of the cooling fluid outlet temperature during the freezing process, and more nodules have finally solidified with a lesser value of b.

4.3. Solidification process simulation

With the heat exchange between the fluid and the nodules going on, the initially liquid PCM gradually solidifies and finally a few nodules turn into solid as seen in Figs. 6 and 7. Most of the nodules in the first Continuous Stirred Tank Reactor begin to solidify in less than 4 h, but only few of them have finished by the end of 15 h. This demonstrates that the solidification step takes much more time than the liquid phase cooling step.

One can define number densities over the whole storage tank as follows:

$$\psi_x(x,t) = \sum_{k=1}^{N} \psi_x^k(x,t)$$
$$\psi_{T_s}(T_s,t) = \sum_{k=1}^{N} \psi_{T_s}^k(T_s,t) \quad (34)$$

Table 1
Parameters used in the model.

Symbol	Description	Value
D_t	Tank diameter (m)	0.5
H_t	Tank height (m)	2.6
q_f	Fluid flow rate ($m^3\ h^{-1}$)	1.57
r_e	External radius of nodules (mm)	49
r_i	Internal radius of nodules (mm)	47.4
n_t	Total nodules number	1900
Δh_{sl}	Fusion enthalpy ($kJ\ kg^{-1}$)	333
c_{pl}	Specific heat of liquid water ($J\ K^{-1}\ kg^{-1}$)	4217
c_{ps}	Specific heat of ice ($J\ K^{-1}\ kg^{-1}$)	2060
c_{pf}	Specific heat of cooling fluid ($J\ K^{-1}\ kg^{-1}$)	3589
a_s	Thermal diffusivity of ice ($10^{-6}\ m^2\ s^{-1}$)	1.2
a_l	Thermal diffusivity of liquid water ($10^{-6}\ m^2\ s^{-1}$)	0.13
λ_{env}	Thermal conductivity of envelope ($W\ m^{-1}\ K^{-1}$)	0.43

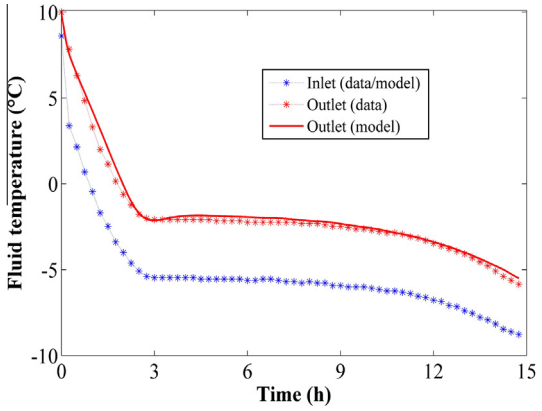

Fig. 3. Comparison of predicted and experimental outlet cooling fluid temperature.

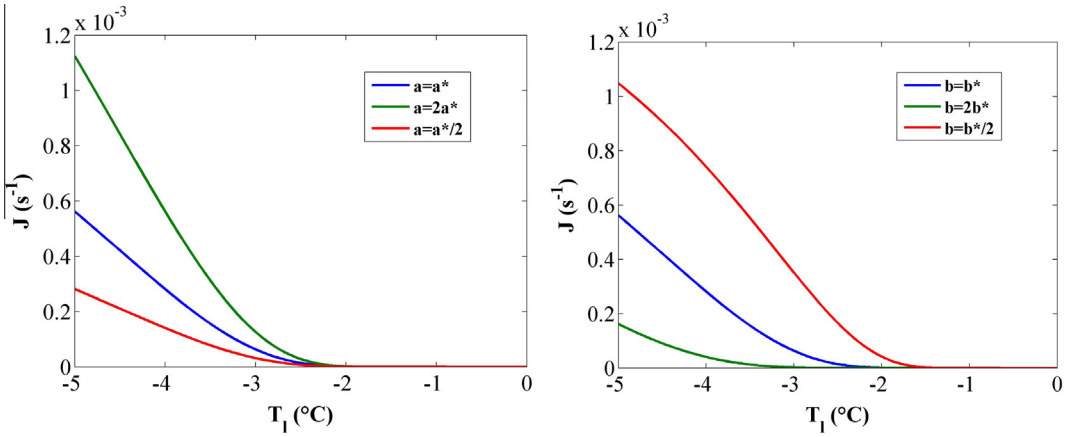

Fig. 4. Probability of crystallization J for different values of a and b.

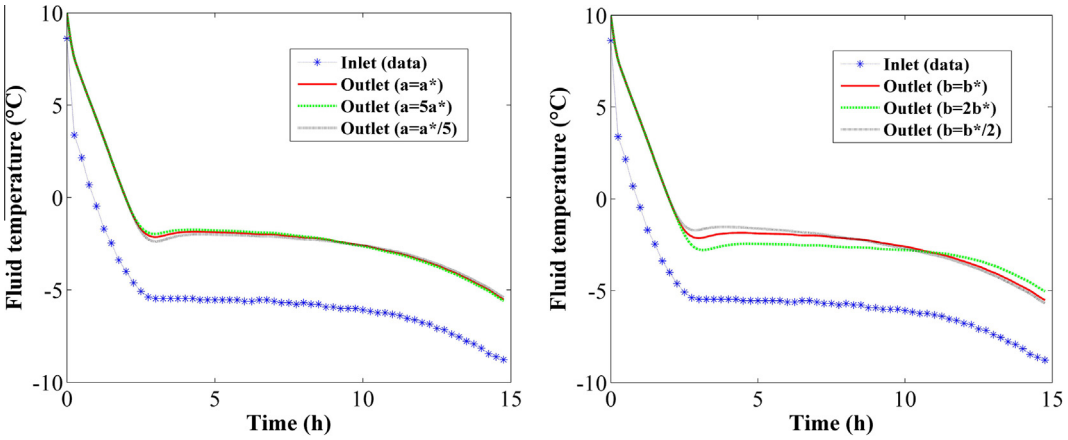

Fig. 5. Calculated cooling fluid outlet temperature for different values of a and b.

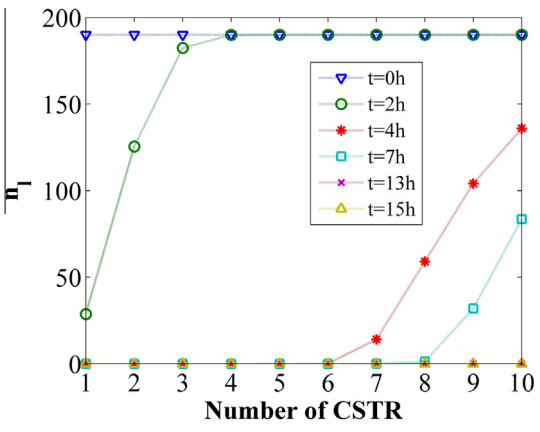

Fig. 6. Calculated profiles of liquid nodules number at various time.

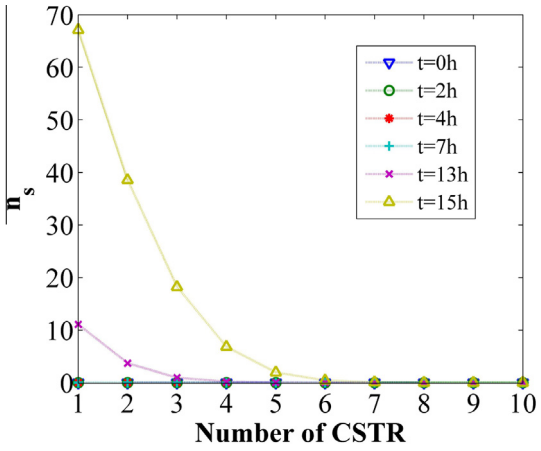

Fig. 7. Calculated profiles of entirely solidified nodules number at various time.

These distributions are depicted in Figs. 8 and 9. We see that the peak of the density according to the mass fraction moves from $x = 0$ to $x = 1$, which describes the evolution of the global solid mass fraction during the charging process. As seen in Fig. 8, once upon the PCM has entirely solidified, the mean solid phase temperature begins to decrease significantly.

In order to globally quantify the solidification process, let us define $\gamma^k(t)$ as the mean solid phase mass fraction within the k^{th} Continuous Stirred Tank Reactor and $\gamma(t)$ the one over the whole storage tank:

$$\begin{cases} \gamma^k(t) = \dfrac{\int_\varepsilon^1 \psi_x^k(x,t)x\,dx + \int_{T_{s,\min}}^{Tm} \psi_{T_s}^k(T_s,t)dT_s}{n_t^k} \\ \gamma(t) = \dfrac{\int_\varepsilon^1 \psi_x(x,t)x\,dx + \int_{T_{s,\min}}^{Tm} \psi_{T_s}(T_s,t)dT_s}{\sum_{k=1}^N n_t^k} \end{cases} \tag{35}$$

$\gamma = \gamma^k = 0$ when the content of all the nodules under consideration is liquid, and $\gamma = \gamma^k = 1$ when the content of all the nodules under consideration is entirely solidified.

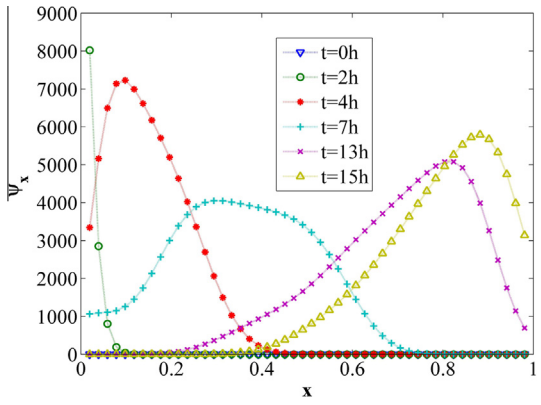

Fig. 8. Calculated distribution of the number density of nodules containing a solid–liquid mixture at various time in the entire storage.

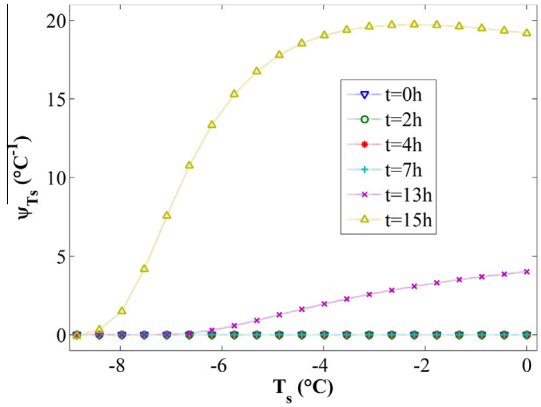

Fig. 9. Calculated distribution of the number density of nodules containing solid phase at various time in the entire storage.

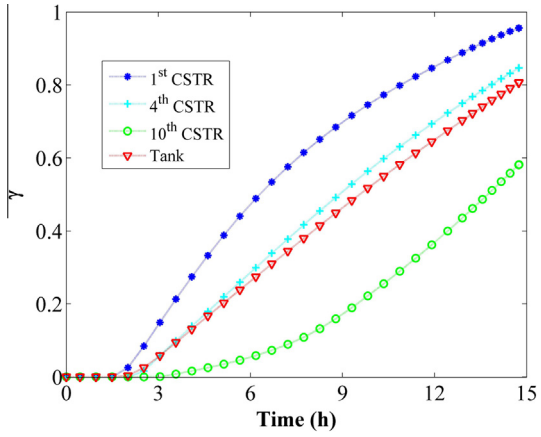

Fig. 10. Calculated evolutions of mean solid mass fraction in different Continuous Stirred Tank Reactors and in the whole tank.

The evolutions of γ with time in different Continuous Stirred Tank Reactors and in the whole tank are presented in Fig. 10. Considering that the fluid absorbs heat as it flows through the nodules, its cooling capacity decreases along the flow direction. Therefore the mean solid mass fraction drops along the flow direction as well. In this case, the solidification process is not entirely complete during the charging process, and approximately 80% of the total mass of PCM has been finally solidified.

5. Conclusions

In this paper a novel dynamic model to simulate the charging process of cold energy storage tank using population balance equations is presented. Through characterizing the system state by the distribution of the nodules associated with different properties, the dynamic of the system is represented by the evolution of nodules number density. The supercooling phenomenon is taken into account in the model by using a nucleation rate model which permits to represent the stochastic character of the solidification during the cooling process. The transitions between different nodules states are taken as boundary conditions for the population balance equations, so the evolution of the system state is continuous and it is unnecessary to account for discrete events related to the transitions.

The model is validated by comparing the model predictions with experimental data. The simulation provides good results of the evolution of the storage cooling fluid outlet temperature, and the other calculated results are pertinent as well. As far as we know, it is the first time that this population balance equations approach is used for PCM thermal storage modeling.

Conflict of interest

The authors have no conflict of interest to declare.

Acknowledgements

This work has been funded by the French National Research Agency (ANR) within the framework of the project ANR-11-SEED-0004-02 ACLIRSYS (Advanced Control for Low Inertia Refrigeration Systems).

Appendix A. The Linear Driving Force Glueckauf model

As given by Carslaw and Jaeger [37], the mean temperature $\overline{T}(t)$ of a sphere of radius r that is subject to transient heat conduction and a step variation of its surface temperature can be expressed as:

$$\overline{T}(t) = T_0 + (T_i - T_0)\left(1 - \frac{6}{\pi^2}\sum_{n=1}^{\infty}\frac{1}{n^2}\exp\left(-\frac{n^2\pi^2 a}{r^2}t\right)\right) \quad \text{(A-1)}$$

where T_0 is the initial uniform temperature within the sphere and T_i the constant surface temperature. Glueckauf [35] has transposed this transient heat conduction problem into a transient diffusion problem. Actually, one can continue to apply this approach to the transient heat conduction problem. If T_i varies over time, one can calculate $\overline{T}(t)$ by using Duhamel's theorem [38] and then calculate its variation over time $\frac{d\overline{T}}{dt}$ as:

$$\frac{d\overline{T}}{dt} = \frac{6a}{r^2}\int_{\tau=0}^{\tau=t}\frac{dT_i}{d\tau}\sum_{n=1}^{\infty}\exp(-\frac{n^2\pi^2 a}{r^2}t)d\tau \quad \text{(A-2)}$$

By performing successive integration by parts and assuming a rapid convergence of the series involved in the derivation, Glueckauf [35] has finally obtained:

$$\frac{d\overline{T}}{dt} = \frac{6a}{r^2}\left(\pi^2(T_i - \overline{T}) + \underbrace{\left(1 - \frac{\pi^2}{15}\right)}_{0.342}\frac{dT_i}{dt} - \underbrace{\left(\frac{1}{15} - \frac{2\pi^2}{315}\right)}_{0.0040}\frac{d^2T_i}{dt^2} + \cdots\right) \quad \text{(A-3)}$$

where the terms involving second- and higher order derivatives can usually be neglected. By considering that $\frac{d\overline{T}}{dt} \approx \frac{dT_i}{dt}$, the final form of the Linear Driving Force model is then as follows:

$$\frac{d\overline{T}}{dt} = \frac{15a}{r^2}(T_i - \overline{T}) \tag{A-4}$$

Yao and Tien [39] have shown that the Linear Driving Force model is equivalent to the solution of the unsteady-state conduction equation by using the orthogonal collocation method with one collocation point. They have also shown that the Linear Driving Force expression gives the best approximation (in the least-square sense) if a parabolic temperature profile within the sphere is assumed. In the case of a step response to T_i, the difference between the Linear Driving Force model and the exact solution is less than 4% for a time duration $t > 0.1\frac{r^2}{a}$. In our case, $r = r_i = 47.4$ mm and $a \approx 10^{-6}$ m^2 s^{-1}, so that a good approximation can be obtained for $t > 225$ s. Therefore, the use of the Linear Driving Force model provides a sufficient approximation in our model since the time duration of the storage charge cycle is much longer than necessary (see Fig. 3).

References

[1] D.N. Nkwetta, F. Haghighat, Thermal energy storage with phase change material – a state-of-the art review, Sustain. Cities Soc. 10 (2014) 87–100.
[2] F. Agyenim, N. Hewitt, P. Eames, M. Smyth, A review of materials, heat transfer and phase change problem formulation for latent heat thermal energy storage systems (LHTESS), Renew. Sust. Energy Rev. 14 (2) (2010) 615–628.
[3] G. Zsembinszki, P. Moreno, C. Solé, A. Castell, L. Cabeza, Numerical model evaluation of a PCM cold storage tank and uncertainty analysis of the parameters, Appl. Therm. Eng. 67 (1–2) (2014) 16–23.
[4] V. Martin, B. He, F. Setterwall, Direct contact PCM-water cold storage, Appl. Energy 87 (2010) 2652–2659.
[5] X. Chen, M. Worall, S. Omer, Y. Su, S. Riffat, Experimental investigation on PCM cold storage integrated with ejector cooling system, Appl. Therm. Eng. 63 (2014) 419–427.
[6] Y. Dutil, D.R. Rousse, N.B. Salah, S. Lassue, L. Zalewski, A review on phase-change materials: mathematical modeling and simulations, Renew. Sust. Energy Rev. 15 (2011) 112–130.
[7] P. Verma, S.K. Varun, Singal, Review of mathematical modeling on latent heat thermal energy storage systems using phase-change material, Renew. Sust. Energy Rev. 12 (2008) 999–1031.
[8] S. Liu, Y. Li, Y. Zhang, Mathematical solutions and numerical models employed for the investigations of PCM's phase transformations, Renew. Sust. Energy Rev. 33 (2014) 659–674.
[9] K.A.R. Ismail, J.R. Henriquez, Numerical and experimental study of spherical capsules packed bed latent heat storage system, Appl. Therm. Eng. 22 (2002) 1705–1716.
[10] L. Bilir, Z. Ilken, Total solidification time of a liquid phase change material enclosed in cylindrical/ spherical containers, Appl. Therm. Eng. 25 (2005) 1488–1502.
[11] J. Bony, S. Citherlet, Numerical model and experimental validation of heat storage with phase change materials, Energy Build. 39 (2007) 1065–1072.
[12] E.V. Votyakov, A.M. Bonanos, A perturbation model for stratified thermal energy storage tanks, Int. J. Heat Mass Transfer 75 (2014) 218–223.
[13] S. Zhang, J. Niu, Experimental investigation of effects of super-cooling on microencapsulated phase-change material (MPCM) slurry thermal storage capacities, Sol. Energy Mater. Sol. Cells 94 (2010) 1038–1048.
[14] T. Kousksou, T. El Rhafiki, K. El Omari, Y. Zeraouli, Y. Le Guer, Forced convective heat transfer in supercooled phase-change material suspensions with stochastic crystallization, Int. J. Refrig 33 (2010) 1569–1582.
[15] S. Wu, G. Fang, X. Liu, Thermal performance simulations of a packed bed cool thermal energy storage system using n-tetradecane as phase change material, Int. J. Therm. Sci. 49 (2010) 1752–1762.
[16] N. Calvet, X. Py, R. Olivès, J.P. Bédécarrats, J.P. Dumas, F. Jay, Enhanced performances of macro-encapsulated phase change materials (PCMs) by intensification of the internal effective thermal conductivity, Energy 55 (2013) 956–964.
[17] D. Clausse, J.P. Dumas, P.H.E. Meijer, F. Broto, Phase transformations in emulsions. Part I: Effects of thermal treatments on nucleation phenomena: experiments and model, J. Disper. Sci. Technol. 8 (1) (1987) 1–28.
[18] J.P. Bédécarrats, F. Strub, B. Falcon, J.P. Dumas, Phase-change thermal energy storage using spherical capsules: performance of a test plant, Int. J. Refrig 19 (1996) 187–196.
[19] T. Kousksou, J.P. Bédécarrats, J.P. Dumas, A. Mimet, Dynamic modelling of the storage of an encapsulated ice tank, Appl. Therm. Eng. 25 (10) (2005) 1534–1548.
[20] J.P. Bédécarrats, J. Castaing-Lasvignottes, F. Strub, J.P. Dumas, Study of a phase change energy storage using spherical capsules. Part II: Numerical modelling, Energy Convers. Manage. 50 (2009) 2537–2546.
[21] T. El Rhafiki, T. Kousksou, A. Jamil, S. Jegadheeswaran, S.D. Pohekar, Y. Zeraouli, Crystallization of PCMs inside an emulsion: supercooling phenomenon, Sol. Energy Mat. Sol. C 95 (2011) 2588–2597.
[22] R.B. Bird, W.E. Stewart, E.N. Lightfoot, Transport Phenomena, Revised second ed., Wiley, 2006.
[23] D. Ramkrishna, Population Balances: Theory and Applications to Particulate Systems in Engineering, Academic Press, San Diego, 2000. pp. 15–22.
[24] C. Kotoulas, C. Kiparissides, A generalized population balance model for the prediction of particle size distribution in suspension polymerization reactors, Chem. Eng. Sci. 61 (2006) 332–346.
[25] C.Y. Ma, X.Z. Wang, Model identification of crystal facet growth kinetics in morphological population balance modeling of L-glutamic acid crystallization and experimental validation, Chem. Eng. Sci. 70 (2012) 22–30.
[26] P.J. Becker, F. Puel, H.A. Jakobsen, N. Sheibat-Othman, Development of an improved breakage kernel for high dispersed viscosity phase emulsification, Chem. Eng. Sci. 109 (2014) 326–338.
[27] F. Puel, G. Fevotte, J.P. Klein, Simulation and analysis of industrial crystallization processes through multidimensional population balance equations. Part 1: A resolution algorithm based on the method of classes, Chem. Eng. Sci. 58 (2003) 3715–3727.
[28] M. Oullion, F. Puel, G. Fevotte, S. Righini, P. Carvin, Industrial batch crystallization of a plate-like organic product. In situ Monitoring and 2D-CSD modelling. Part 2: Kinetic modelling and identification, Chem. Eng. Sci. 62 (2007) 833–845.
[29] D. Turnbull, Solid State Physics III, Academic Press, New York, 1956. pp. 225–306.
[30] D. Kashchiev, N. Kaneko, K. Sato, Kinetics of crystallization in polydisperse emulsions, J. Colloid Interf. Sci. 208 (1998) 167–177.
[31] N. Wakao, S. Kaguei, Heat and Mass Transfer in Packed beds, Gordon and Breach, Science Publishers, New York, 1982. pp. 264–295.
[32] Y. Zhu, Y. Zhang, Dynamic modeling of encapsulated ice tank for HVAC system simulation, HVAC&R Res. 6 (3) (2000) 213–228.
[33] D.M. Ruthven, Principle of Adsorption and Adsorption Processes, John Wiley and Sons, New York, 1984.
[34] D. Leinekugel-le-Coq, M. Tayakout-Fayolle, Y. Legorrec, C. Jallut, A double linear driving force approximation for non-isothermal mass transfer modeling through bi-disperse adsorbents, Chem. Eng. Sci. 62 (15) (2007) 4040–4053.
[35] E. Glueckauf, Theory of chromatography Part 10: Formula for diffusion into spheres and their application to chromatography, Trans. Faraday Soc. 51 (1955) 1540–1551.
[36] J.P. Bédécarrats, J. Castaing-Lasvignottes, F. Strub, J.P. Dumas, Study of a phase change energy storage using spherical capsules. Part I: Experimental results, Energy Convers. Manage. 50 (2009) 2527–2536.
[37] H.S. Carslaw, J.C. Jaeger, Conduction of Heat in Solids, Oxford University Press, Oxford, 1947.
[38] M.N. Ozisik, Heat Conduction, John Wiley and Sons, New York, 1993.
[39] C. Yao, C. Tien, Approximation of intraparticle mass transfer in adsorption processes-I. Linear systems, Chem. Eng. Sci. 47 (2) (1992) 457–464.